Creating Accurate Multivariate Rational Interpolation Models of Microwave Circuits by Using Efficient Adaptive Sampling to Minimize the Number of Computational Electromagnetic Analyses

Robert Lehmensiek, *Student Member, IEEE*, and Petrie Meyer, *Member, IEEE*

***Abstract*—A fast and efficient adaptive sampling algorithm for multivariate rational interpolation models based on convergents of Thiele-type branched continued fractions (BCFs) is presented in this paper. We propose a variation of the standard BCF that uses approximation to establish a nonrectangular grid of support points. Starting with a low-order interpolant, the technique systematically increases the order by optimally choosing new support points in the areas of highest error until the required accuracy is achieved. In this way, accurate surrogate models are established by a small number of support points without any *a priori* knowledge of the data. The technique is evaluated on several passive microwave structures.**

***Index Terms*—Computer-aided design, model-based parameter estimation, multivariate adaptive sampling, multivariate rational interpolation, surrogate modeling.**

I. Introduction

MICROWAVE design incorporating optimization, Monte Carlo analysis, or statistical computer-aided design relies on fast and accurate analyses or models of physical structures to be effective. Computational electromagnetic (CEM) analysis techniques normally provide high accuracy at the expense of computational effort, while circuit models, if they exist, are computationally very effective, but lack wide-band accuracy. Surrogate mathematical models, directly fitting data from CEM simulations, offer fast and accurate solutions to this problem, and are increasingly used in the design of microwave components [1], [2]. Current models include lookup tables, interpolation techniques, and artificial neural networks. Lookup tables employ low-order polynomial interpolation between entries in a multidimensional (normally uniform) grid [3]. They require an exponentially increasing amount of storage space as the dimension increases, and struggle to model nonlinearities. Artificial neural networks can model highly nonlinear functions with high dimensionality, but require networks with the right topology, high numbers of training and testing examples, and often excessive training times. They do, however, require only the coefficients of the network to be stored and, once trained, are very fast to evaluate [4], [5]. Interpolation techniques also require only storage of the interpolant coefficients and, in addition, normally require the smallest amount of data to establish a model [6]–[8]. Several authors have applied the interpolation technique to the method of moments, for which derivatives with respect to frequency can be calculated and integrated into the interpolation model [9]–[11].

While polynomial interpolants are often used, rational functions yield better results for functions containing poles or for meromorphic functions. Polynomial interpolation is prone to wild oscillations and an acceptable accuracy is sometimes achieved only by polynomials of intolerably high degree [12], [13]. A rational function can be constructed by calculating the explicit solution of a system of interpolatory conditions, by starting a recursive algorithm, or by calculating the convergent of a continued fraction [14], [15]. The use of continued fractions as interpolants is a computationally efficient method [16] and gives accurate numerical results [17], [18]. Recursive algorithms, on the other hand, are accurate, but determine the value of the interpolant directly for a single value from tabulated data without calculating the coefficients. Hence, they become computationally inefficient for a large number of function evaluations. This method was used in [19]. The technique of solving a system of interpolatory conditions, while used most often [9]–[11], [19]–[24], is generally accepted to be the least accurate method.

The extension of univariate interpolation to multivariate interpolation is not trivial since a large degree of freedom in the choice for the numerator and denominator polynomials exists. Only a few multivariate sampling algorithms have been published. In [19], the authors use a rectangular grid of support points and recursive univariate interpolation to establish the multidimensional interpolation space. They also mention establishing a multivariate function by solving a linear system of equations. In [23], multivariate polynomials are used to build a model for the geometrical parameters at a single frequency and rational interpolation is used to combine these polynomials to determine the entire interpolation space.

The orders of interpolants are generally determined heuristically or estimated [10], [20], [22]. With no *a priori* knowledge of the problem, this can easily lead to overdetermined interpolants, requiring high numbers of support points. When CEM

Manuscript received December 9, 2000.

R. Lehmensiek is with Reutech Radar Systems, Stellenbosch 7600, South Africa and also with the Department of Electrical and Electronic Engineering, University of Stellenbosch, 7602 Stellenbosch, South Africa.

P. Meyer is with the Department of Electrical and Electronic Engineering, University of Stellenbosch, 7602 Stellenbosch, South Africa.

Publisher Item Identifier S 0018-9480(01)06134-8.

techniques are used for the generation of the support points, it is of utmost importance to minimize the required number, especially in the multivariate case. This can only be achieved by the use of adaptive sampling schemes, where the order of the function is gradually increased until a desired accuracy is reached. In turn, this requires that a suitable error function exists and that unequally spaced support points can be used [25]. Published error functions include the difference between two interpolation models that either use different data sample sets and/or are of different rational polynomial orders [19], [20], [22], [23].

In this paper, a novel adaptive sampling algorithm for general multivariate interpolation based on a Thiele-type branched continued fraction (BCF) representation of a rational function is presented. The proposed technique is based on a recently published adaptive sampling algorithm for univariate interpolation [26] and constructs sets of single-parameter interpolants at optimal points in a $(D-1)$-variable space. Starting with low-order interpolants, the technique systematically increases the order by optimally choosing new support points in the areas of highest error, until the required accuracy is achieved. The univariate interpolants are, in turn, used to form bivariate, trivariate, and finally D-variable functions, establishing accurate surrogate models from a small number of support points. The standard BCF interpolation technique, which requires a fully filled rectangular grid of support points, is adapted here to allow sampling on a nonrectangular grid. Support points are, therefore, placed optimally in the interpolation space with the result of a reduction in the number of CEM analysis. The coefficients of the rational interpolant and the evaluation of the function values are determined in a recursive manner, making the adaptive algorithm fast and efficient. An error estimate is obtained as a natural consequence of the recursion. Support points are selected efficiently to create accurate surrogate models without oversampling the interpolation space. The algorithm is fully automatic, does not require derivatives, is widely applicable, and is in no way restricted to the specific examples shown here. The accuracy of the technique, which depends on the number of support points, is illustrated by two- and three-variable examples, with errors of smaller than 0.25% being achieved in all cases. This model accuracy is more than sufficient for the purposes of designing most microwave circuits.

The multivariate interpolation used in this paper has, as starting point, the more simple univariate rational interpolation. In order to ease understanding of the former, both the formulation of the interpolant and the adaptive sampling algorithm for the univariate case will first be discussed briefly (see [26] and [27] for details). The detailed expositions of the new algorithms for the multivariate case, together with results, make up the bulk of this paper.

II. Univariate Rational Interpolation

Rational interpolation defines an analytic function $\Re$ of the complex variable γ as a quotient of two polynomials $N_\zeta(\gamma)$ and $D_\nu(\gamma)$

$$\Re(\gamma) = \frac{N_\zeta(\gamma)}{D_\upsilon(\gamma)} = \frac{\sum_{k=0}^{\zeta} p_k \gamma^k}{\sum_{k=0}^{\upsilon} q_k \gamma^k} \tag{1}$$

with ζ being the order of the numerator, ν being the order of the denominator, and p_k and q_k being the polynomial coefficients. The rational interpolant $\Re$ provides an approximation on an interval $[\gamma^{(0)}, \gamma^{(1)}]$ of the function $S(\gamma)$ that we are trying to model. Since there are $\zeta + \nu + 1$ unknown coefficients (q_0 is chosen arbitrarily), a set of $N+1 = \zeta + \nu + 1$ support points $(\gamma^{(i)}; S_i)$, with $i = 0, 1, \ldots, N$ and $S_i = S(\gamma^{(i)})$, are required to completely determine $\Re(\gamma)$. $\Re(\gamma)$ is then a curve passing through the ordinates S_i at the abscissas $\gamma^{(i)}$ for $i = 0, 1, \ldots, N$. We assume $\Re(\gamma)$ exists and has no unattainable support points [28]. A simple test can be added to test for unattainable support points.

Equation (1) is represented by a convergent of a corresponding Thiele continued fraction, as shown in (2). Each rational expression $\Re_k(\gamma)$ is a kth-order partial fraction expansion of (1), together constituting a set of interpolants that exhibit increasing accuracy as k increases, reaching a convergent value at $k = N$.

$$\begin{aligned}
&\Re_k(\gamma) \\
&= S_0 + \cfrac{\gamma - \gamma^{(0)}}{\varphi_1\left(\gamma^{(1)}, \gamma^{(0)}\right) + \cfrac{\gamma - \gamma^{(1)}}{\varphi_2\left(\gamma^{(2)}, \gamma^{(1)}, \gamma^{(0)}\right) + \cdots \cfrac{}{\cdots + \cfrac{\gamma - \gamma^{(k-1)}}{\varphi_k\left(\gamma^{(k)}, \gamma^{(k-1)}, \ldots, \gamma^{(0)}\right)}}}} \\
&= S_0 + \sum_{i=1}^{k} \frac{\gamma - \gamma^{(i-1)}}{\varphi_i\left(\gamma^{(i)}, \gamma^{(i-1)}, \ldots, \gamma^{(0)}\right)}, \\
&\qquad k = 0, 1, \ldots, N.
\end{aligned} \tag{2}$$

The inverse differences φ_k are the partial denominators of (2) and are essentially the coefficients that define $\Re_k(\gamma)$. The inverse differences are determined recursively from the support points, defined in (3), shown at the bottom of this page [29].

The interpolation function $\Re_k(\gamma)$ can be evaluated numerically with the three-term recurrence relations given in (4) initialized with $N_0(\gamma) = S_0$, $D_0(\gamma) = 1$, $N_1(\gamma) =$

$$\begin{aligned}
\varphi_1\left(\gamma^{(i)}, \gamma^{(0)}\right) &\equiv \frac{\gamma^{(i)} - \gamma^{(0)}}{S_i - S_0}, \qquad i = 1, 2, \ldots, N \\
\varphi_k\left(\gamma^{(i)}, \gamma^{(k-1)}, \ldots, \gamma^{(0)}\right) &\equiv \frac{\gamma^{(i)} - \gamma^{(k-1)}}{\varphi_{k-1}\left(\gamma^{(i)}, \gamma^{(k-2)}, \ldots, \gamma^{(0)}\right) - \varphi_{k-1}\left(\gamma^{(k-1)}, \gamma^{(k-2)}, \ldots, \gamma^{(0)}\right)}, \qquad i = k, k+1, \ldots, N; \\
&\qquad k = 2, 3, \ldots, N.
\end{aligned} \tag{3}$$

$\varphi_1(\gamma^{(1)}, \gamma^{(0)})N_0(\gamma) + (\gamma - \gamma^{(0)})$, and $D_1(\gamma) = \varphi_1(\gamma^{(1)}, \gamma^{(0)})$ [30].

$$\left.\begin{aligned} N_k(\gamma) &= \varphi_k\left(\gamma^{(k)}, \gamma^{(k-1)}, \ldots, \gamma^{(0)}\right) \\ &\quad \cdot N_{k-1}(\gamma) + (\gamma - \gamma^{(k-1)})N_{k-2}(\gamma) \\ D_k(\gamma) &= \varphi_k\left(\gamma^{(k)}, \gamma^{(k-1)}, \ldots, \gamma^{(0)}\right) \\ &\quad \cdot D_{k-1}(\gamma) + \left(\gamma - \gamma^{(k-1)}\right)D_{k-2}(\gamma) \\ &\quad k = 2, 3, \ldots, N \end{aligned}\right\},$$

$$\Re_k(\gamma) = \frac{N_k(\gamma)}{D_k(\gamma)}, \qquad k = 0, 1, \ldots, N. \tag{4}$$

Recursive equations are also available for the derivative of $\Re_k(\gamma)$ with respect to γ. The computational effort in determining the coefficients $\varphi_k(\gamma_k, \gamma_{k-1}, \ldots, \gamma_0)$ for $k = 1, 2, \ldots, N$ using the recurrence relations in (3) is $N(N+1)/2$ divisions and $N(N+1)$ subtractions. To evaluate $N_N(\gamma)$ or $D_N(\gamma)$ with the recurrence relations in (4) requires $2N - 1$ multiplications, N additions, and N subtractions. In total, to evaluate $\Re_N(\gamma)$ requires $4N - 2$ multiplications, one division, $2N$ additions, and $2N$ subtractions.

III. Univariate Adaptive Sampling

The determination of an accurate rational interpolant requires that enough support points, in the case of microwave circuits, normally CEM analyses, be used. In order to calculate the minimum number and the optimal positions of these support points, an adaptive sampling algorithm for application to the rational function approximation was proposed in [26], and briefly explained here for clarity. The technique has successfully been applied to various microwave problems [26], [27].

Starting with the rational interpolation formulation, a natural residual term emerges as

$$E_k(\gamma) = \frac{\left|\Re_k(\gamma) - \Re_{k-1}(\gamma)\right|^2}{\left(1 + \left|\Re_k(\gamma)\right|\right)^2}$$

which provides an estimate of the interpolation error. This is the relative squared error between the current estimate of the interpolant and the previous estimate of the interpolant, i.e., before adding the last support point. The adaptive algorithm is defined to work in the interval $[\gamma^{(0)}, \gamma^{(1)}]$. As a first step, an arbitrary third support point $\gamma^{(2)}$ is selected, which lies in the interval $[\gamma^{(0)}, \gamma^{(1)}]$. The values for S_k at these points are determined by CEM analysis. The residual $E_2(\gamma)$ is now evaluated at a large number of equispaced sample points in the interval $[\gamma^{(0)}, \gamma^{(2)}]$. The interval $[\gamma^{(2)}, \gamma^{(1)}]$, i.e., the interval in which the last support point was placed, is ignored, as it does not provide a suitable error estimate. At the maximum of the evaluated sample points, a new support point $\gamma^{(3)}$ is selected, thereby minimizing the residual. The process is repeated until the residual becomes arbitrarily small. It is important to note that, for a full iteration, only one point is determined via a CEM analysis. As all the other computation steps only require the evaluation of the interpolation function, the computational effort is decreased substantially. Fig. 1 shows a step in the execution of the algorithm, with the new sample point indicated with an asterisk.

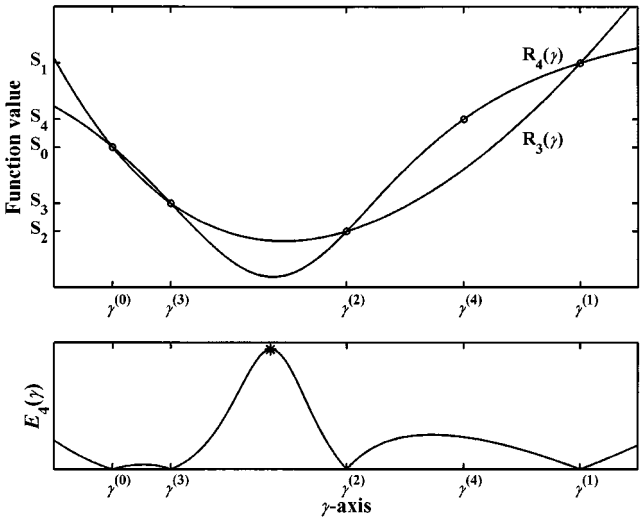

Fig. 1. Illustration of the adaptive sampling technique. The interpolation functions $\Re_3(\gamma)$, $\Re_4(\gamma)$, and the residual $E_4(\gamma)$ are shown. The asterisk indicates the new sample point.

The adaptive sampling algorithm automatically selects and minimizes the number of support points, and it does not require any *a priori* knowledge of the dynamics of the function in order to define an interpolation model $\Re(\gamma)$. The following important points should be noted.

1) The number of equispaced evaluations of the residual is not crucial as long as it is of an order larger than the number of support points.
2) For highly nonlinear functions, the number of support points can become large, causing the order of the rational polynomial to become large and the algorithm to become numerically unstable. To prevent this, the interval is subdivided when N reaches its critical value [27].
3) As a consequence of the continued fraction formulation for k even $\zeta = \upsilon = k/2$ and for k odd $\zeta = (k+1)/2$ and $\upsilon = (k-1)/2$.
4) Equiripple error can only be achieved if the function is known, in which case, economization [13] or, specifically, a Remes-type algorithm [31] can be used.
5) As the accuracy of the interpolant is required to increase, the accuracy of the CEM analysis technique needs to increase. Otherwise, the interpolation process will try to model the error of the CEM analysis because it determines an interpolant and not an approximant, and this will lead to an excessive number of support points being selected.

IV. Multivariate Rational Interpolation

The multivariate rational function is defined in (5), where γ_d with $d = 1, 2, \ldots, D$ represents the D complex variables. The interpolation function $\Re(\gamma_1, \gamma_2, \ldots, \gamma_D)$ will be equal to the function $S(\gamma_1, \gamma_2, \ldots, \gamma_D)$, which we are trying to model, at the support points and will approximate $S(\gamma_1, \gamma_2, \ldots, \gamma_D)$ between the support points. A set of support points required to determine $\Re(\gamma_1, \gamma_2, \ldots, \gamma_D)$ are

represented by $(\gamma_1^{(i_1)}, \gamma_2^{(i_2)}, \ldots, \gamma_D^{(i_D)};\ S_{i_1,i_2,\ldots,i_D})$, where $i_d = 0, 1, \ldots, N_d$, $d = 1, 2, \ldots, D$, and $S_{i_1,i_2,\ldots,i_D} = S(\gamma_1^{(i_1)}, \gamma_2^{(i_2)}, \ldots, \gamma_D^{(i_D)})$. For the moment, we assume that the support points are placed on a fully filled not necessarily equidistant rectangular grid and, therefore, the full set is given by the Cartesian product of the support points for each variable, i.e.,

$$\left\{\gamma_1^{(0)}, \gamma_1^{(1)}, \ldots, \gamma_1^{(N_1)}\right\} \times \left\{\gamma_2^{(0)}, \gamma_2^{(1)}, \ldots, \gamma_2^{(N_2)}\right\} \times \cdots \times \left\{\gamma_D^{(0)}, \gamma_D^{(1)}, \ldots, \gamma_D^{(N_D)}\right\}.$$

We will use a method analogous to the univariate case for determination and evaluation of the multivariate rational interpolant. The generic equations for our multivariate rational interpolation technique are given in the following paragraphs.

$$\Re(\gamma_1, \gamma_2, \ldots, \gamma_D) = \frac{N(\gamma_1, \gamma_2, \ldots, \gamma_D)}{D(\gamma_1, \gamma_2, \ldots, \gamma_D)}. \tag{5}$$

The interpolation function $\Re(\gamma_1, \gamma_2, \ldots, \gamma_D)$ is represented by the convergent of a multivariate Thiele-type BCF of the form

$$\Re(\gamma_1, \gamma_2, \ldots, \gamma_D) = \Re_0\left(\gamma_2, \gamma_3, \ldots, \gamma_D \middle| \gamma_1^{(0)}\right) + \sum_{i_1=1}^{N_1} \frac{\gamma_1 - \gamma_1^{(i_1-1)}}{\left|\ \Re_{i_1}\left(\gamma_2, \gamma_3, \ldots, \gamma_D \middle| \gamma_1^{(i_1)}\right)\right.}. \tag{6}$$

Compared to the univariate continued fraction in (2), each of the constant partial denominators is replaced with a multivariate function $\Re_{i_1}(\gamma_2, \gamma_3, \ldots, \gamma_D|\gamma_1^{(i_1)})$, which has one less variable than $\Re(\gamma_1, \gamma_2, \ldots, \gamma_D)$ and is defined with γ_1 constant and equal to $\gamma_1^{(i_1)}$. Each $\Re_{i_1}(\gamma_2, \gamma_3, \ldots, \gamma_D|\gamma_1^{(i_1)})$ can, in turn, be represented by a continued fraction, where $\Re_{i_2}(\gamma_3, \gamma_4, \ldots, \gamma_D|\gamma_1^{(i_1)}, \gamma_2^{(i_2)})$ is defined at $\gamma_1 = \gamma_1^{(i_1)}$ and $\gamma_2 = \gamma_2^{(i_2)}$:

$$\Re_{i_1}\left(\gamma_2, \gamma_3, \ldots, \gamma_D \middle| \gamma_1^{(i_1)}\right) = \Re_0\left(\gamma_3, \gamma_4, \ldots, \gamma_D \middle| \gamma_1^{(i_1)}, \gamma_2^{(0)}\right) + \sum_{i_2=1}^{N_2} \frac{\gamma_2 - \gamma_2^{(i_2-1)}}{\left|\ \Re_{i_2}\left(\gamma_3, \gamma_4, \ldots, \gamma_D \middle| \gamma_1^{(i_1)}, \gamma_2^{(i_2)}\right)\right.}, \quad i_1 = 0, 1, \ldots, N_1. \tag{7}$$

The substitution of the partial denominators by continued fractions is repeatedly performed according to (8). The number of variables of $\Re_{i_d}(\gamma_{d+1}, \gamma_{d+2}, \ldots, \gamma_D|\gamma_1^{(i_1)}, \gamma_2^{(i_2)}, \ldots, \gamma_d^{(i_d)})$ decreases with every step until this function becomes a univariate function $\Re_{i_d}(\gamma_D|\gamma_1^{(i_1)}, \gamma_2^{(i_2)}, \ldots, \gamma_{D-1}^{(i_{D-1})})$, in which case, (3) is used to determine the coefficients and (4) is used to evaluate $\Re_{i_d}(\gamma_D|\gamma_1^{(i_1)}, \gamma_2^{(i_2)}, \ldots, \gamma_{D-1}^{(i_{D-1})})$.

$$\Re_{i_{d-1}}\left(\gamma_d, \gamma_{d+1}, \ldots, \gamma_D \middle| \gamma_1^{(i_1)}, \gamma_2^{(i_2)}, \ldots, \gamma_{d-1}^{(i_{d-1})}\right) = \Re_0\left(\gamma_{d+1}, \gamma_{d+2}, \ldots, \gamma_D \middle| \gamma_1^{(i_1)}, \gamma_2^{(i_2)}, \ldots, \gamma_d^{(0)}\right) + \sum_{i_d=1}^{N_d} \frac{\gamma_d - \gamma_d^{(i_d-1)}}{\left|\ \Re_{i_d}\left(\gamma_{d+1}, \gamma_{d+2}, \ldots, \gamma_D \middle| \gamma_1^{(i_1)}, \gamma_2^{(i_2)}, \ldots, \gamma_d^{(i_d)}\right)\right.}, \quad i_{d-1} = 0, 1, \ldots, N_{d-1};\quad d = 2, 3, \ldots, D-1. \tag{8}$$

The computation of the above multivariate continued fraction follows a tree-like structure and is, therefore, called a BCF. Different forms of BCFs can be constructed, depending on the way in which the list of support points is enumerated [32]–[34]. The BCF used here was defined by Siemaszko [35].

Similar to the univariate case, each of the BCFs of (6)–(8) can be evaluated by using three-term recurrence relations given in (9) for $d = 1, 2, \ldots, D-1$, initialized with

$$\begin{aligned}
&N_0(\gamma_d, \gamma_{d+1}, \ldots, \gamma_D) = \Re_0\left(\gamma_{d+1}, \gamma_{d+2}, \ldots, \gamma_D \middle| \gamma_1^{(i_1)}, \gamma_2^{(i_2)}, \ldots, \gamma_d^{(0)}\right)\\
&D_0(\gamma_d, \gamma_{d+1}, \ldots, \gamma_D) = 1\\
&N_1(\gamma_d, \gamma_{d+1}, \ldots, \gamma_D) = \Re_1\left(\gamma_{d+1}, \gamma_{d+2}, \ldots, \gamma_D \middle| \gamma_1^{(i_1)}, \gamma_2^{(i_2)}, \ldots, \gamma_d^{(1)}\right) \cdot N_0(\gamma_d, \gamma_{d+1}, \ldots, \gamma_D) + \left(\gamma_d - \gamma_d^{(0)}\right)
\end{aligned}$$

and

$$D_1(\gamma_d, \gamma_{d+1}, \ldots, \gamma_D) = \Re_1\left(\gamma_{d+1}, \gamma_{d+2}, \ldots, \gamma_D \middle| \gamma_1^{(i_1)}, \gamma_2^{(i_2)}, \ldots, \gamma_d^{(1)}\right).$$

$$\left.\begin{aligned}
&N_k(\gamma_d, \gamma_{d+1}, \ldots, \gamma_D)\\
&\quad = \Re_k\left(\gamma_{d+1}, \gamma_{d+2}, \ldots, \gamma_D \middle| \gamma_1^{(i_1)}, \gamma_2^{(i_2)}, \ldots, \gamma_d^{(k)}\right)\\
&\qquad \cdot N_{k-1}(\gamma_d, \gamma_{d+1}, \ldots, \gamma_D) + \left(\gamma_d - \gamma_d^{(k-1)}\right)\\
&\qquad \cdot N_{k-2}(\gamma_d, \gamma_{d+1}, \ldots, \gamma_D)\\
&D_k(\gamma_d, \gamma_{d+1}, \ldots, \gamma_D)\\
&\quad = \Re_k\left(\gamma_{d+1}, \gamma_{d+2}, \ldots, \gamma_D \middle| \gamma_1^{(i_1)}, \gamma_2^{(i_2)}, \ldots, \gamma_d^{(k)}\right)\\
&\qquad \cdot D_{k-1}(\gamma_d, \gamma_{d+1}, \ldots, \gamma_D) + \left(\gamma_d - \gamma_d^{(k-1)}\right)\\
&\qquad \cdot D_{k-2}(\gamma_d, \gamma_{d+1}, \ldots, \gamma_D)
\end{aligned}\right\}, \quad k = 2, 3, \ldots, N_d$$

$$\Re_k\left(\gamma_d, \gamma_{d+1}, \ldots, \gamma_D \middle| \gamma_1^{(i_1)}, \gamma_2^{(i_2)}, \ldots, \gamma_{d-1}^{(i_{d-1})}\right) = \frac{N_k(\gamma_d, \gamma_{d+1}, \ldots, \gamma_D)}{D_k(\gamma_d, \gamma_{d+1}, \ldots, \gamma_D)}, \qquad k = 0, 1, \ldots, N_d. \quad (9)$$

In this case, sets of support points are combined to define sets of univariate interpolation functions with $D-1$ variables constant. The union of these univariate interpolation functions then generates sets of bivariate functions. Sets of bivariate functions combine to form three-variable interpolation functions. The process is repeated until a multivariate interpolation function with D variables is determined.

From the above formulation, it follows that the determination of the coefficients for the multivariate interpolant is equivalent to the determination of coefficients for a set of univariate functions. These univariate functions are determined by repeatedly applying the set of recurrence relations given in (10), shown at the bottom of this page, for $d = 1, 2, \ldots, D-1$. Then,

$$\Re_{i_d}\left(\gamma_{d+1}, \gamma_{d+2}, \ldots, \gamma_D \middle| \gamma_1^{(i_1)}, \gamma_2^{(i_2)}, \ldots, \gamma_d^{(i_d)}\right) = \xi_{i_d}\left(\gamma_d^{(i_d)}, \gamma_d^{(i_d-1)}, \ldots, \gamma_d^{(0)}; \gamma_{d+1}, \gamma_{d+2}, \ldots, \gamma_D\right), \quad i_d = 0, 1, \ldots, N_d. \quad (11)$$

Note that the evaluation of (10) requires all the support points in $\{\gamma_1^{(0)}, \gamma_1^{(1)}, \ldots, \gamma_1^{(N_1)}\} \times \{\gamma_2^{(0)}, \gamma_2^{(1)}, \ldots, \gamma_2^{(N_2)}\} \times \cdots \times \{\gamma_D^{(0)}, \gamma_D^{(1)}, \ldots, \gamma_D^{(N_D)}\}$, as assumed at the beginning of this section. This constriction of a rectangular grid of support points, which is an inherent characteristic of BCFs, is not suited for an adaptive sampling algorithm that requires the freedom to choose arbitrary support points in the interpolation space. Furthermore, we expect that a number of the support points in the grid are redundant.

An important step to enable an adaptive scheme to be applied can now be taken. The constriction of the rectangular grid is removed by approximating certain function values with the previously determined interpolants for those functions when evaluating $\xi_{i_d}(\gamma_d^{(i_d)}, \gamma_d^{(i_d-1)}, \ldots, \gamma_d^{(0)}; \gamma_{d+1}, \gamma_{d+2}, \ldots, \gamma_D)$. Equation (10), for $d = 1, 2, \ldots, D-1$, therefore, becomes (12), shown at the bottom of the following page, and (11) becomes

$$\Re_{i_d}\left(\gamma_{d+1}, \gamma_{d+2}, \ldots, \gamma_D \middle| \gamma_1^{(i_1)}, \gamma_2^{(i_2)}, \ldots, \gamma_d^{(i_d)}\right) = \zeta_{i_d}\left(\gamma_d^{(i_d)}, \gamma_d^{(i_d-1)}, \ldots, \gamma_d^{(0)}; \gamma_{d+1}, \gamma_{d+2}, \ldots, \gamma_D\right), \quad i_d = 0, 1, \ldots, N_d. \quad (13)$$

This simple procedure makes a world of difference, as the rectangularly spaced support points required by the BCF can now effectively be calculated from nonrectangularly spaced support points. The following important points should be noted.

1) Since the number of support points for each univariate function may be different according to (12), the orders of the BCFs, N_d, for $d = 2, 3, \ldots, D$, are now functions of their positions, i.e., $N_d^{(i_1, i_2, \ldots, i_{d-1})}$, and for implementation, (7)–(9) and (12) need to be adapted.
2) Since each multivariate interpolant is the construct of a set of lower dimensional interpolants, it is important to ensure that the accuracy of these lower dimensional interpolants increases as the number of variables decreases.
3) The degree sets of the numerator and the denominator polynomials are completely determined by the form of the BCF, which, in turn, is determined by the structure of the support points.
4) Different numberings of the support points produces different interpolants with dissimilar accuracies [17]. Interpolants are more accurate when the support points are renumbered so that the orders of the BCFs decrease for increasing branches of the BCF.

V. Multivariate Adaptive Sampling

The multivariate rational interpolation formulation given in Section IV is essentially univariate in nature. Therefore, we

$$\begin{aligned}
&\xi_0\left(\gamma_d^{(i)}; \gamma_{d+1}, \gamma_{d+2}, \ldots, \gamma_D\right) \equiv S\left(\gamma_1^{(i_1)}, \gamma_2^{(i_2)}, \ldots, \gamma_d^{(i)}, \gamma_{d+1}, \ldots, \gamma_D\right) \\
&\xi_1\left(\gamma_d^{(i)}, \gamma_d^{(0)}; \gamma_{d+1}, \gamma_{d+2}, \ldots, \gamma_D\right) \equiv \frac{\gamma_d^{(i)} - \gamma_d^{(0)}}{\xi_0\left(\gamma_d^{(i)}; \gamma_{d+1}, \gamma_{d+2}, \ldots, \gamma_D\right) - \xi_0\left(\gamma_d^{(0)}; \gamma_{d+1}, \gamma_{d+2}, \ldots, \gamma_D\right)}, \qquad i = 1, 2, \ldots, N_d \\
&\xi_k\left(\gamma_d^{(i)}, \gamma_d^{(k-1)}, \ldots, \gamma_d^{(0)}; \gamma_{d+1}, \gamma_{d+2}, \ldots, \gamma_D\right) \equiv \frac{\gamma_d^{(i)} - \gamma_d^{(k-1)}}{\xi_{k-1}\left(\gamma_d^{(i)}, \gamma_d^{(k-2)}, \ldots, \gamma_d^{(0)}; \gamma_{d+1}, \gamma_{d+2}, \ldots, \gamma_D\right) - \xi_{k-1}\left(\gamma_d^{(k-1)}, \gamma_d^{(k-2)}, \ldots, \gamma_d^{(0)}; \gamma_{d+1}, \gamma_{d+2}, \ldots, \gamma_D\right)}, \\
&\qquad i = k, k+1, \ldots, N_d; \quad k = 2, 3, \ldots, N_d. \quad (10)
\end{aligned}$$

can apply an adaptive sampling algorithm similar to that used for the univariate case. Two different adaptive sampling algorithms are considered. The first algorithm, based on (10) and (11), determines a set of support points in the interpolation space placed on a fully filled (not equidistant) rectangular grid. The second algorithm places support points on a nonrectangular grid and is based on (12) and (13). The interpolation space is defined in $\gamma_d \in [\gamma_d^{(0)}, \gamma_d^{(1)}]$ for $d = 1, 2, \ldots, D$. At initialization, an arbitrary set of points $\gamma_d^{(2)}$ are selected in the interval $[\gamma_d^{(0)}, \gamma_d^{(1)}]$.

An estimate of the interpolation error for the partial interpolants of (8) is given in (14), shown at the bottom of this page. The function $E_k(\gamma_d, \gamma_{d+1}, \ldots, \gamma_D | \gamma_1^{(i_1)}, \gamma_2^{(i_2)}, \ldots, \gamma_{d-1}^{(k)})$ is only defined for the variable γ_d, with $\gamma_{d+1}, \gamma_{d+2}, \ldots, \gamma_D$ defining the position at which the error function can be evaluated. To reduce the computational effort required in evaluating (14), especially for a larger number of variables, $E_k(\gamma_d, \gamma_{d+1}, \ldots, \gamma_D | \gamma_1^{(i_1)}, \gamma_2^{(i_2)}, \ldots, \gamma_{d-1}^{(k)})$ is only evaluated at $\gamma_{d+1} = \gamma_{d+1}^{(2)}, \gamma_{d+2} = \gamma_{d+2}^{(2)}, \ldots, \gamma_D = \gamma_D^{(2)}$. Practical examples have shown that $E_k(\gamma_d, \gamma_{d+1}, \ldots, \gamma_D | \gamma_1^{(i_1)}, \gamma_2^{(i_2)}, \ldots, \gamma_{d-1}^{(k)})$ is largely independent of the variables $\gamma_{d+1}, \gamma_{d+2}, \ldots, \gamma_D$, provided that $\Re_k(\gamma_d, \gamma_{d+1}, \ldots, \gamma_D | \gamma_1^{(i_1)}, \gamma_2^{(i_2)}, \ldots, \gamma_{d-1}^{(k)})$ is accurate for all k. Due to the renumbering of the support points, as mentioned in Section IV, it is necessary that an error function be zero at all of the support points in order to be able to place a new support point at the maximum of this error function. Evaluation of the error function in (14), with the support points in the series $\{\gamma_d^{(0)}, \gamma_d^{(1)}, \ldots, \gamma_d^{(N_d)}\}$, will determine a function that is zero at all of the support points, except at $\gamma_d^{(N_d)}$. A different error function can be defined, which is zero at all of the support points, except at $\gamma_d^{(N_d-1)}$, when the last two support points in the series are swapped around. A new error function, defined as the product of the square root of the above two error functions, is zero at all of the support points. Although the same method can be applied to the univariate case, this has no benefit.

The first multivariate adaptive sampling algorithm, denoted ASA1, determines the multivariate rational interpolant as shown in the following steps.

Step 1) Using the univariate adaptive sampling algorithm, determine a univariate model of each variable γ_d over the interval $[\gamma_d^{(0)}, \gamma_d^{(1)}]$, with all other variables set to their midpoint values, i.e., $\gamma_m = \gamma_m^{(0)} + (\gamma_m^{(1)} - \gamma_m^{(0)})/2$ for $m = 1, 2, \ldots, D$ and $m \neq d$. In this way, D univariate interpolants and their respective sets of support points, each lying on a line crossing through the center of the interpolation space, are determined.

Step 2) Sort the variable positions in the multivariate interpolant so that the orders N_d of the interpolants determined in step 1) decrease as d increases in (8).

$$
\begin{aligned}
&\zeta_0\left(\gamma_d^{(i)}; \gamma_{d+1}, \gamma_{d+2}, \ldots, \gamma_D\right) \\
&\quad \equiv S\left(\gamma_1^{(i_1)}, \gamma_2^{(i_2)}, \ldots, \gamma_d^{(i)}, \gamma_{d+1}, \ldots, \gamma_D\right) \\
&\zeta_1\left(\gamma_d^{(i)}, \gamma_d^{(0)}; \gamma_{d+1}, \gamma_{d+2}, \ldots, \gamma_D\right) \\
&\quad \equiv \frac{\gamma_d^{(i)} - \gamma_d^{(0)}}{\zeta_0\left(\gamma_d^{(i)}; \gamma_{d+1}, \gamma_{d+2}, \ldots, \gamma_D\right) - \Re_0\left(\gamma_{d+1}, \gamma_{d+2}, \ldots, \gamma_D \middle| \gamma_1^{(i_1)}, \gamma_2^{(i_2)}, \ldots, \gamma_d^{(0)}\right)}, \qquad i = 1, 2, \ldots, N_d \\
&\zeta_k\left(\gamma_d^{(i)}, \gamma_d^{(k-1)}, \ldots, \gamma_d^{(0)}; \gamma_{d+1}, \gamma_{d+2}, \ldots, \gamma_D\right) \\
&\quad \equiv \frac{\gamma_d^{(i)} - \gamma_d^{(k-1)}}{\zeta_{k-1}\left(\gamma_d^{(i)}, \gamma_d^{(k-2)}, \ldots, \gamma_d^{(0)}; \gamma_{d+1}, \gamma_{d+2}, \ldots, \gamma_D\right) - \Re_{k-1}\left(\gamma_{d+1}, \gamma_{d+2}, \ldots, \gamma_D \middle| \gamma_1^{(i_1)}, \gamma_2^{(i_2)}, \ldots, \gamma_d^{(k-1)}\right)}, \\
&\qquad i = k, k+1, \ldots, N_d; \quad k = 2, 3, \ldots, N_d
\end{aligned}
\tag{12}
$$

$$
\begin{aligned}
&E_k\left(\gamma_d, \gamma_{d+1}, \ldots, \gamma_D \middle| \gamma_1^{(i_1)}, \gamma_2^{(i_2)}, \ldots, \gamma_{d-1}^{(k)}\right) \\
&\quad = \frac{\left|\Re_k\left(\gamma_d, \gamma_{d+1}, \ldots, \gamma_D \middle| \gamma_1^{(i_1)}, \gamma_2^{(i_2)}, \ldots, \gamma_{d-1}^{(k)}\right) - \Re_{k-1}\left(\gamma_d, \gamma_{d+1}, \ldots, \gamma_D \middle| \gamma_1^{(i_1)}, \gamma_2^{(i_2)}, \ldots, \gamma_{d-1}^{(k-1)}\right)\right|^2}{\left(1 + \left|\Re_k\left(\gamma_d, \gamma_{d+1}, \ldots, \gamma_D \middle| \gamma_1^{(i_1)}, \gamma_2^{(i_2)}, \ldots, \gamma_{d-1}^{(k)}\right)\right|\right)^2}
\end{aligned}
\tag{14}
$$

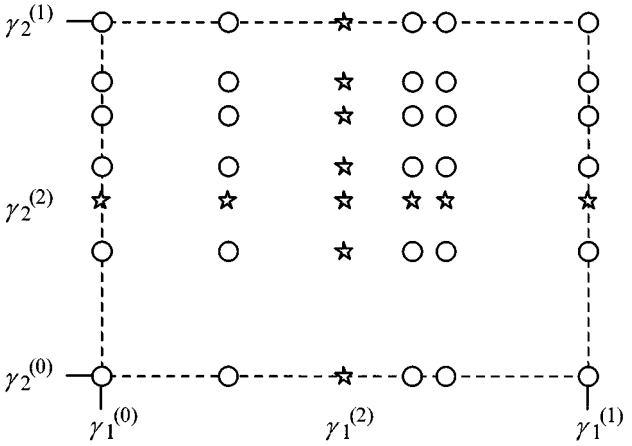

Fig. 2. Illustration of the support point placement using ASA1.

Step 3) Generate a rectangular grid of support points from the points determined in step 1), i.e., all the points in $\{\gamma_1^{(0)}, \gamma_1^{(1)}, \ldots, \gamma_1^{(N_1)}\} \times \{\gamma_2^{(0)}, \gamma_2^{(1)}, \ldots, \gamma_2^{(N_2)}\} \times \cdots \times \{\gamma_D^{(0)}, \gamma_D^{(1)}, \ldots, \gamma_D^{(N_D)}\}$.

Step 4) Determine a multivariate rational interpolant from the grid of support points defined in step 3) using (10), (11), and (3).

We expound ASA1 by means of a bivariate example illustrated in Fig. 2. Step 1) of the algorithm determines the star-shaped support points by means of a univariate interpolation along the dimensions γ_1 and γ_2 at $\gamma_2^{(2)}$ and $\gamma_1^{(2)}$, respectively. Since $N_1 = 6$ is smaller than $N_2 = 7$ in the example, γ_1 and γ_2 are exchanged in the interpolant. Hence, the interpolant $\Re(\gamma_2, \gamma_1)$ consists of a union of univariate interpolants $\Re(\gamma_1)$. In step 3), a grid of support points is generated by adding the circle-shaped support points, as shown in Fig. 2. $\Re(\gamma_2, \gamma_1)$ is determined from this rectangular grid of support points.

The second multivariate adaptive sampling algorithm, denoted ASA2, determines the multivariate rational interpolant as shown in the following steps.

Step 1) Same as for ASA1.

Step 2) Same as for ASA1.

Step 3) Initialize a model with a rectangular grid of support points with three support points along every dimension, i.e., 3^D support points in $\{\gamma_1^{(0)}, \gamma_1^{(1)}, \gamma_1^{(2)}\} \times \{\gamma_2^{(0)}, \gamma_2^{(1)}, \gamma_2^{(2)}\} \times \cdots \times \{\gamma_D^{(0)}, \gamma_D^{(1)}, \gamma_D^{(2)}\}$.

Step 4) Determine a multivariate rational interpolant from the support points using (12), (13), and (3).

Step 5) Select a dimension γ_d for selection of new support points. Iterate for $d = D, D-1, \ldots, 1$.

Step 6) Select a new support point at the maximum of the error function at γ_d.

Step 7) Renumber the support points so that N_d decreases as d increases.

Step 8) Repeat steps 4)–8) until convergence.

We expound ASA2 by means of a bivariate example illustrated in Fig. 3. Steps 1) and 2) are the same as in ASA1. We assume N_2 is smaller than N_1. In step 3), an initialization grid of nine support points is generated, as shown by the star-shaped support points in Fig. 3(a). $\Re(\gamma_1, \gamma_2)$ is determined from these nine support points. Using the univariate adaptive sampling algorithm, we completely determine $\Re_0(\gamma_2)$ with a predetermined accuracy by placing support points at $\gamma_1^{(0)}$. We then determine $\Re_1(\gamma_2)$ at $\gamma_1^{(1)}$. Since $N_2^{(0)} = 7$ is bigger than $N_2^{(1)} = 6$, we continue by determining $\Re_1(\gamma_2)$ at $\gamma_1^{(2)}$. With $N_2^{(2)} = 8$, we renumber the support points so that the support points at $\gamma_1^{(2)}$ determine $\Re_0(\gamma_2)$, the support points at $\gamma_1^{(0)}$ determine $\Re_1(\gamma_2)$, the support points at $\gamma_1^{(1)}$ determine $\Re_2(\gamma_2)$ in (6) and, hence, $\gamma_1^{(0)}$, $\gamma_1^{(1)}$, and $\gamma_1^{(2)}$ become $\gamma_1^{(1)}$, $\gamma_1^{(2)}$, and $\gamma_1^{(0)}$, respectively, as shown in Fig. 3(b). We then evaluate the error function for γ_1 at $\gamma_2^{(2)}$ and determine $\gamma_1^{(3)}$ at the maximum of this error. We initialize $\Re_3(\gamma_2)$ with three support points at $\gamma_2^{(0)}$, $\gamma_2^{(1)}$ and $\gamma_2^{(2)}$, shown by the star-shaped support points in Fig. 3(b). Using the univariate adaptive sampling algorithm, we completely determine $\Re_3(\gamma_2)$ at $\gamma_1^{(3)}$. The process is repeated until the error function has reached its predetermined accuracy.

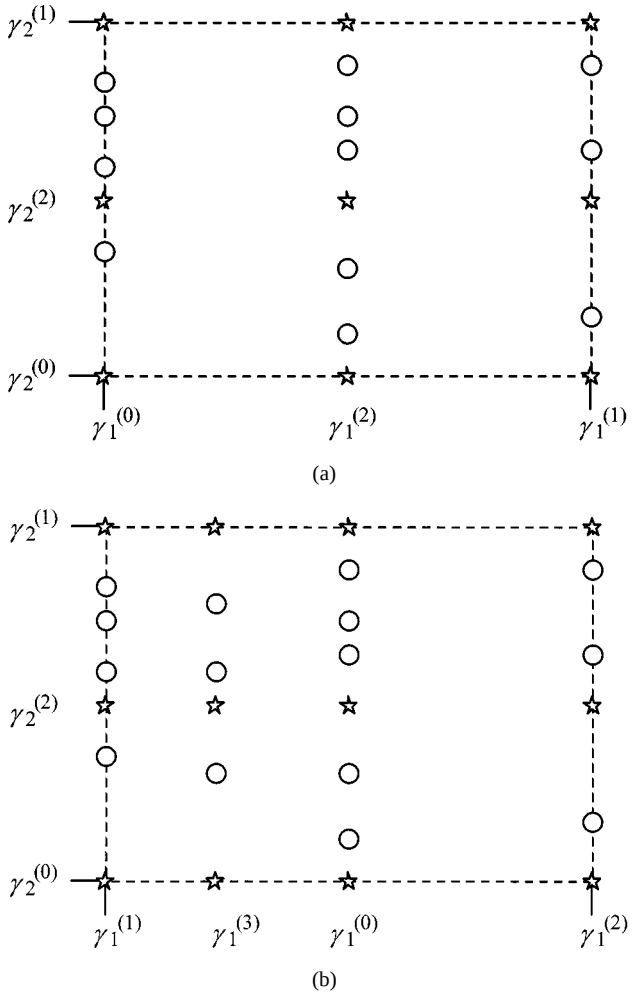

Fig. 3. Illustration of the support point placement using ASA2. (a) After three steps. (b) After the fourth step.

If required, interval subdivision, as mentioned in Section III for the univariate case, is applied to the variable γ_D.

VI. Examples

To verify the algorithms discussed in Sections IV and V, a number of two- and three-dimensional models were created for standard microwave circuits. To determine the accuracy of the

TABLE I
CONVERGENCE OF $\Re(\text{w/h}, \varepsilon_r)$ DETERMINED BY ASA1 AND ASA2 FOR THE STRIPLINE EXAMPLE

ASA1			ASA2		
Number of support points	$E_m(\text{w/h}, \varepsilon_r)$ [dB]		Number of support points	$E_m(\text{w/h}, \varepsilon_r)$ [dB]	
	Mean	Max		Mean	Max
9	−29.3	−16.4	9	−29.3	−16.4
16	−40.4	−25.9	14	−33.0	−18.5
24	−42.4	−30.0	21	−42.4	−29.1
36	−74.5	−58.8	29	−72.3	−56.9

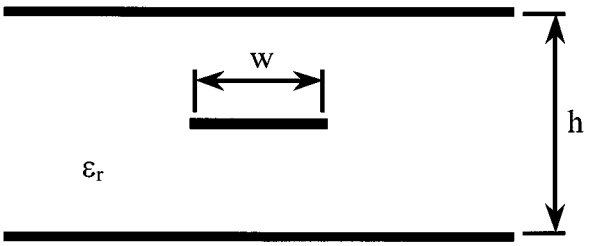

Fig. 4. Cross-sectional view of the stripline.

models, they have to be evaluated on an independent evaluation data set, similar to the validation procedures applied to neural networks. In the following examples, the relative squared error E_m between the function and the model on a 30^2 equispaced grid for the bivariate cases and on a 20^3 equispaced grid for the trivariate cases was calculated. In all cases, both the maximum and average errors in decibels are shown for models of varying size. None of these models were reduced in size after a fit was obtained, in contrast to techniques where the order of the interpolant is guessed beforehand, and the interpolation function (calculated by a high number of CEM analyses) is systematically reduced afterwards.

A. Stripline Characteristic Impedance—Two Variables

A bivariate model $\Re(\text{w/h}, \varepsilon_r)$ was determined with the adaptive sampling algorithm for the characteristic impedance $Z_0(\text{w/h}, \varepsilon_r)$ of a homogeneous symmetric stripline, as shown in Fig. 4. The variables are the strip width-to-height (w/h) ratio and the relative dielectric constant ε_r of the substrate. The strip conductor was assumed infinitesimally thin, thus $Z_0(\text{w/h}, \varepsilon_r)$ can be computed using the exact formula, which is derived using a conformal transformation [36]. The model is determined for the parameters $\text{w/h} \in [0.05, 1]$ and $\varepsilon_r \in [1, 25]$, which define the interpolation space. At initialization, the nine chosen support points produce $\Re(\text{w/h}, \varepsilon_r)$ with the maximum error equal to -16.4 dB. Table I shows the convergence of the models using ASA1 and ASA2 as the number of support points increase. With equivalent accuracies (-57 dB), the model determined by ASA2 required seven less support points than ASA1. The response of the interpolation model $\Re(\text{w/h}, \varepsilon_r)$ with 29 support points determined with ASA2 and its relative squared error $E_m(\text{w/h}, \varepsilon_r)$, which is less than -56 dB in the interpolation space, are shown in Figs. 5 and 6, respectively.

B. Capacitive Step in Rectangular Waveguide—Two Variables

Bivariate models $\Re_{11}(f, h)$ and $\Re_{21}(f, h)$, and $\Re_{11}(f, l)$ and $\Re_{21}(f, l)$, were determined for the reflection and transmission coefficients, i.e., $S_{11}(f, h)$ and $S_{21}(f, h)$, and $S_{11}(f, l)$ and $S_{21}(f, l)$, of a capacitive step in a rectangular waveguide, as shown in Fig. 7. The variables are frequency f and gap height h, and frequency f and gap length l. The models were determined for a standard WR90 rectangular waveguide. The capacitive step was analyzed using the mode-matching method combined with the generalized scattering matrix [37]. The models $\Re_{11}(f, h)$ and $\Re_{21}(f, h)$ are determined with $f \in [7\text{ GHz}, 13\text{ GHz}]$, $h \in [2\text{ mm}, 8\text{ mm}]$ and $l = 2$ mm. Tables II and III show the con-

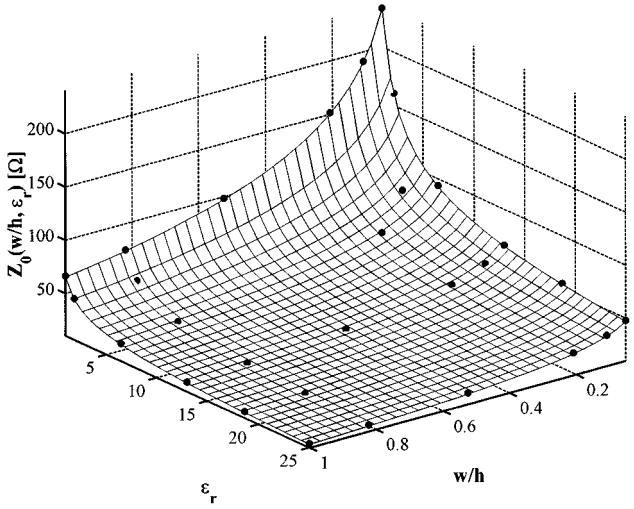

Fig. 5. ASA2: stripline example. Response of $\Re(\text{w/h}, \varepsilon_r)$ with 29 support points.

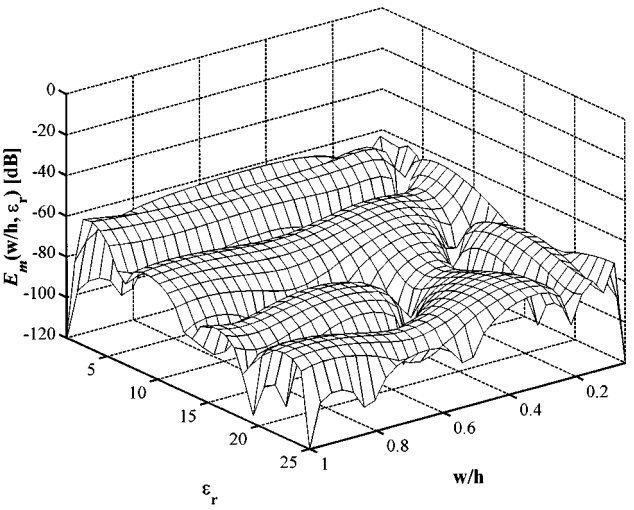

Fig. 6. ASA2: stripline example. $E_m(\text{w/h}, \varepsilon_r)$ of $\Re(\text{w/h}, \varepsilon_r)$ with 29 support points.

TABLE II
CONVERGENCE OF $\Re_{11}(f, h)$ DETERMINED BY ASA1 AND ASA2 FOR THE CAPACITIVE STEP EXAMPLE

ASA1			ASA2		
Number of support points	E_{11}(f, h) [dB] Mean	Max	Number of support points	E_{11}(f, h) [dB] Mean	Max
12	−34.4	−20.3	15	−52.5	−35.4
16	−54.5	−45.7	20	−61.4	−44.9
20	−57.5	−45.0	22	−62.5	−48.2
30	−68.2	−50.5	37	−76.2	−51.1
42	−81.0	−70.1	44	−93.2	−82.3

TABLE III
CONVERGENCE OF $\Re_{21}(f, h)$ DETERMINED BY ASA1 AND ASA2 FOR THE CAPACITIVE STEP EXAMPLE

ASA1			ASA2		
Number of support points	E_{21}(f, h) [dB] Mean	Max	Number of support points	E_{21}(f, h) [dB] Mean	Max
12	−51.3	−38.0	13	−52.3	−44.8
15	−52.3	−38.0	18	−61.8	−51.9
25	−65.3	−53.6	22	−64.6	−28.4
35	−82.2	−61.2	37	−91.5	−71.3
42	−90.1	−78.5	44	−94.1	−80.7

TABLE IV
CONVERGENCE OF $\Re_{11}(f, l)$ AND $\Re_{21}(f, l)$ DETERMINED BY ASA2 FOR THE CAPACITIVE STEP EXAMPLE

$\Re_{11}$(f, l)			$\Re_{21}$(f, l)		
Number of support points	E_{11}(f, l) [dB] Mean	Max	Number of support points	E_{21}(f, l) [dB] Mean	Max
12	−42.3	−22.1	12	−54.8	−38.0
17	−57.1	−40.2	16	−56.7	−36.2
21	−61.1	−50.7	19	−65.6	−51.8
45	−82.5	−63.8	42	−89.3	−71.1

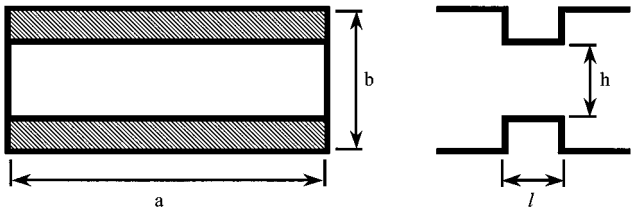

Fig. 7. Cross-sectional view and side view of the capacitive step.

vergence of the models using ASA1 and ASA2 as the number of support points increase. The models $\Re_{11}(f, l)$ and $\Re_{21}(f, l)$ are determined with $f \in [7\text{ GHz}, 13\text{ GHz}]$, $l \in [0.5\text{ mm}, 5\text{ mm}]$ and $h = 5$ mm. Table IV shows the convergence of the models using ASA2 as the number of support points increase. With an equivalent number of support points, the errors of the models determined by ASA2 tend to be less by up to 10 dB compared to those determined by ASA1.

C. Inductive Posts in Rectangular Waveguide—Two Variables

Bivariate models $\Re_{11}(f, w)$ and $\Re_{21}(f, w)$ were determined for the reflection and transmission coefficients, i.e., $S_{11}(f, w)$ and $S_{21}(f, w)$, of two perfectly conducting round posts centered in the E-plane of a rectangular waveguide, as shown in Fig. 8. The variables are frequency f and post-spacing w. The diameter of the posts d was set to 2 mm and the model was determined for a standard WR90 rectangular waveguide with $f \in [7\text{ GHz}, 13\text{ GHz}]$ and $w \in [4\text{ mm}, 18\text{ mm}]$. A moment-method technique is used to analyze this structure [38]. Tables V and VI show the convergence of the models $\Re_{11}(f, w)$ and $\Re_{21}(f, w)$ using ASA1 and ASA2 as the number of support points increase.

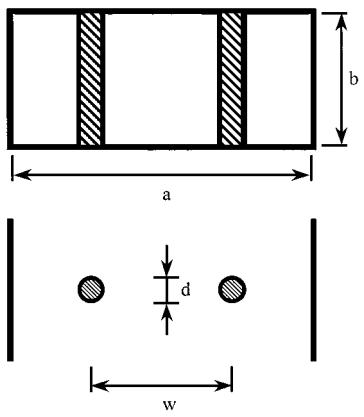

Fig. 8. Cross-sectional view and top view of the inductive posts.

D. Capacitive Step in Rectangular Waveguide—Three Variables

A trivariate model $\Re_{11}(f, h, l)$ was determined for the reflection coefficient, i.e., $S_{11}(f, h, l)$ of a capacitive step in a

TABLE V
CONVERGENCE OF $\Re_{11}(f, w)$ DETERMINED BY ASA1 AND ASA2 FOR THE INDUCTIVE POSTS EXAMPLE

ASA1			ASA2		
Number of support points	E_{11}(f, w) [dB]		Number of support points	E_{11}(f, w) [dB]	
	Mean	Max		Mean	Max
18	−32.4	−16.8	18	−38.1	−23.7
36	−39.8	−13.8	28	−67.2	−49.2
48	−88.4	−73.8	53	−91.5	−73.7

TABLE VI
CONVERGENCE OF $\Re_{21}(f, w)$ DETERMINED BY ASA1 AND ASA2 FOR THE INDUCTIVE POSTS EXAMPLE

ASA1			ASA2		
Number of support points	E_{21}(f, w) [dB]		Number of support points	E_{21}(f, w) [dB]	
	Mean	Max		Mean	Max
18	−38.1	−25.1	23	−59.1	−41.6
36	−39.6	−9.2	30	−52.1	−27.4
48	−89.8	−68.6	51	−76.8	−51.3
56	−90.4	−64.9	57	−87.9	−72.5

TABLE VII
CONVERGENCE OF $\Re_{11}(f, h, l)$ DETERMINED BY ASA1 FOR THE CAPACITIVE STEP EXAMPLE

f ∈ [8 GHz, 12 GHz], h ∈ [3 mm, 7 mm], l ∈ [1 mm, 4 mm]			f ∈ [7 GHz, 13 GHz], h ∈ [2 mm, 8 mm], l ∈ [0.5 mm, 5 mm]		
Number of support points	E_{11}(f, h, l) [dB]		Number of support points	E_{11}(f, h, l) [dB]	
	Mean	Max		Mean	Max
64	−65.1	−49.5	150	−56.6	−31.1
180	−82.2	−55.5	294	−62.0	−30.1
294	−85.3	−59.5	576	−59.3	−15.1
512	−100.8	−63.1	1300	−81.0	−32.1
832	−108.2	−76.6	1716	−83.2	−35.0
936	−109.3	−96.8	2730	−70.0	−26.7

TABLE VIII
CONVERGENCE OF $\Re_{11}(f, h, l)$ DETERMINED BY ASA2 FOR THE CAPACITIVE STEP EXAMPLE

f ∈ [8 GHz, 12 GHz], h ∈ [3 mm, 7 mm], l ∈ [1 mm, 4 mm]			f ∈ [7 GHz, 13 GHz], h ∈ [2 mm, 8 mm], l ∈ [0.5 mm, 5 mm]		
Number of support points	E_{11}(f, h, l) [dB]		Number of support points	E_{11}(f, h, l) [dB]	
	Mean	Max		Mean	Max
115	−70.7	−21.9	343	−55.5	−15.3
164	−75.5	−46.7	593	−67.0	−31.4
300	−86.6	−57.8	737	−76.5	−40.0
379	−89.9	−75.8	871	−79.5	−47.0
496	−107.3	−86.0	1375	−91.7	−47.7
645	−108.3	−94.4	1758	−96.1	−54.7
917	−109.1	−97.5	2142	−97.2	−58.1

rectangular waveguide, as shown in Fig. 7. The variables are frequency f, gap height h, and step length l. The model was determined for a standard WR90 rectangular waveguide. The capacitive step is analyzed using the mode-matching method [37]. Two sets of models were determined with different interpolation spaces, i.e., $f \in [8\,\text{GHz}, 12\,\text{GHz}]$, $h \in [3\,\text{mm}, 7\,\text{mm}]$, and $l \in [1\,\text{mm}, 4\,\text{mm}]$, and $f \in [7\,\text{GHz}, 13\,\text{GHz}]$, $h \in [2\,\text{mm}, 8\,\text{mm}]$, and $l \in [0.5\,\text{mm}, 5\,\text{mm}]$. Tables VII and VIII show the results using ASA1 and ASA2, respectively. For the smaller interpolation space, the models determined by ASA1 and ASA2 attain an error smaller than -95 dB with about 920 support points. ASA2 has a faster convergence than ASA1. For the larger interpolation space, ASA1 failed to produce a model with good accuracy due to the nonoptimal placement of the support points, while ASA2 achieved an error of smaller than -58 dB with 2142 support points.

E. Iris in Rectangular Waveguide—Three Variables

A trivariate model $\Re_{21}(f, a, b)$ was determined for the transmission coefficient, i.e., $S_{21}(f, a, b)$ of an iris in a rectangular waveguide, as shown in Fig. 9. The variables are frequency f, gap width a, and gap height b. The model

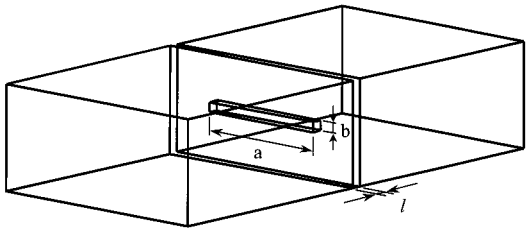

Fig. 9. Iris in rectangular waveguide.

TABLE IX
CONVERGENCE OF $\Re_{21}(f, a, b)$ DETERMINED BY ASA1 FOR THE IRIS EXAMPLE

Number of support points	E_{21}(f, a, b) [dB]	
	Mean	Max
252	−37.9	−3.6
1120	−46.2	−7.4
1440	−44.3	−1.5

TABLE X
CONVERGENCE OF $\Re_{21}(f, a, b)$ DETERMINED BY ASA2 FOR THE IRIS EXAMPLE

Number of support points	E_{21}(f, a, b) [dB]	
	Mean	Max
168	−50.0	−18.0
247	−56.9	−19.5
328	−63.2	−31.1
560	−66.5	−33.1
736	−72.7	−52.6

was determined for a standard WR90 rectangular waveguide with $f \in [8\,\text{GHz}, 12\,\text{GHz}]$, $a \in [8\,\text{mm}, 15\,\text{mm}]$, $b \in [1\,\text{mm}, 3\,\text{mm}]$, and $l = 1$ mm. The iris is analyzed using the mode-matching method [37]. Tables IX and X show the results using ASA1 and ASA2. ASA1 failed to produce a model with good accuracy due to the nonoptimal placement of the support points, while ASA2 achieved an error of smaller than -52 dB with 736 support points.

VII. CONCLUSION

An adaptive sampling algorithm for multivariate rational interpolation based on the Thiele-type BCF has been presented. Support points have been selected efficiently to create accurate mathematical models for the microwave circuits considered. Errors of smaller than 0.25% in the interpolation space were achieved in all cases. The algorithm is fully automatic and does not require any *a priori* knowledge of the microwave structure under study. It does not require derivatives, is widely applicable, and is in no way restricted to the specific examples shown here.

ACKNOWLEDGMENT

The authors wish to thank Prof. A. Cuyt, University of Antwerp, Antwerp, Belgium, for insightful discussions on multivariate rational interpolants.

REFERENCES

[1] A. J. Booker, J. E. Dennis, Jr., P. D. Frank, D. B. Serafini, V. Torczon, and M. W. Trosset, "A rigorous framework for optimization of expensive functions by surrogates," *Structural Optimization*, vol. 17, pp. 1–13, 1999.

[2] E. K. Miller, "Solving bigger problems—By decreasing the operation count and increasing the computation bandwidth," *Proc. IEEE*, vol. 79, no. 10, pp. 1493–1504, Oct. 1990.

[3] V. Rizzoli, A. Costanzo, C. Cecchetti, and D. Masotti, "Computer-aided optimization of broadband nonlinear microwave integrated circuits with the aid of electromagnetically generated look-up tables," *Microwave Opt. Technol. Lett.*, vol. 15, no. 4, pp. 189–196, July 1997.

[4] P. Burrascano, S. Fiori, and M. Mongiardo, "A review of artificial neural networks applications in microwave computer-aided design," in *Int. J. RF Microwave Computer-Aided Eng.*, vol. 9, May 1999, pp. 158–174.

[5] A. H. Zaabab, Q.-J. Zhang, and M. Nakhla, "A neural network modeling approach to circuit optimization and statistical design," *IEEE Trans. Microwave Theory Tech.*, vol. 43, pp. 1349–1358, June 1995.

[6] J. W. Bandler, R. M. Biernacki, S. H. Chen, J. Song, S. Ye, and Q. J. Zhang, "Gradient quadratic approximation scheme for yield-driven design," in *IEEE MTT-S Int. Microwave Symp. Dig.*, Boston, MA, June 1991, pp. 1197–1200.

[7] J.-F. Liang and K. A. Zaki, "CAD of microwave junctions by polynomial curve fitting," in *IEEE MTT-S Int. Microwave Symp. Dig.*, Atlanta, GA, June 1993, pp. 451–454.

[8] J. Carroll and K. Chang, "Statistical computer-aided design for microwave circuits," *IEEE Trans. Microwave Theory Tech.*, vol. 44, pp. 24–32, Jan. 1996.

[9] J. Ureel, N. Faché, D. de Zutter, and P. Lagasse, "Adaptive frequency sampling of scattering parameters obtained by electromagnetic simulation," in *IEEE AP-S Symp. Dig.*, vol. 2, 1994, pp. 1162–1165.

[10] R. S. Adve, T. K. Sarkar, S. M. Rao, E. K. Miller, and D. R. Pflug, "Application of the Cauchy method for extrapolating/interpolating narrow-band system responses," *IEEE Trans. Microwave Theory Tech.*, vol. 45, pp. 837–845, May 1997.

[11] G. J. Burke, E. K. Miller, and S. Chakrabarti, "Using model-based parameter estimation to increase the efficiency of computing electromagnetic transfer functions," *IEEE Trans. Magn.*, vol. 25, pp. 2807–2809, July 1989.

[12] E. G. Kogbetliantz, "Generation of elementary functions," in *Mathematical Methods for Digital Computers*, A. Ralston and H. S. Wilf, Eds. New York: Wiley, 1960, vol. 1.

[13] E. W. Cheney and T. H. Southard, "A survey of methods for rational approximation, with particular reference to a new method based on a formula of Darboux," *SIAM Rev.*, vol. 5, no. 3, pp. 219–231, July 1963.

[14] A. A. M. Cuyt, "A review of multivariate Padé approximation theory," *J. Comput. Appl. Math.*, vol. 12, pp. 221–232, 1985.

[15] A. Cuyt and L. Wuytack, *Nonlinear Methods in Numerical Analysis*, ser. North-Holland Math. Studies: 136, Studies Comput. Math. 1. Amsterdam, The Netherlands: Elsevier, 1987.

[16] P. R. Graves-Morris and T. R. Hopkins, "Reliable rational interpolation," *Numer. Math.*, vol. 36, pp. 111–128, 1981.

[17] A. A. M. Cuyt and B. M. Verdonk, "Multivariate rational interpolation," *Computing*, vol. 34, pp. 41–61, 1985.

[18] A. Cuyt, "A recursive computational scheme for multivariate rational interpolants," *SIAM J. Numer. Anal.*, vol. 24, no. 1, pp. 228–239, Feb. 1987.

[19] S. F. Peik, R. R. Mansour, and Y. L. Chow, "Multidimensional Cauchy method and adaptive sampling for an accurate microwave circuit modeling," *IEEE Trans. Microwave Theory Tech.*, vol. 46, pp. 2364–2371, Dec. 1998.

[20] T. Dhaene, J. Ureel, N. Faché, and D. de Zutter, "Adaptive frequency sampling algorithm for fast and accurate S-parameter modeling of general planar structures," in *IEEE MTT-S Int. Microwave Symp. Dig.*, Orlando, FL, May 1995, pp. 1427–1430.

[21] E. K. Miller, "Model-based parameter estimation in electromagnetics: I—Background and theoretical development," *Appl. Comput. Electromag. Soc. Newslett.*, vol. 10, no. 3, pp. 40–63, Nov. 1995.

[22] ——, "Minimizing the number of frequency samples needed to represent a transfer function using adaptive sampling," in *12th Annu. Rev. Progress Appl. Comput. Electromag.*, Monterey, CA, 1996, pp. 1132–1139.

[23] J. de Geest, T. Dhaene, N. Faché, and D. de Zutter, "Adaptive CAD-model building algorithm for general planar microwave structures," *IEEE Trans. Microwave Theory Tech.*, vol. 47, pp. 1801–1809, Sept. 1999.

[24] D. H. Werner and R. J. Allard, "The simultaneous interpolation of antenna radiation patterns in both the spatial and frequency domains using model-based parameter estimation," *IEEE Trans. Antennas Propagat.*, vol. 48, pp. 383–392, Mar. 2000.
[25] U. Beyer and F. Śmieja, "Data exploration with reflective adaptive models," *Comput. Stat. Data Anal.*, vol. 22, pp. 193–211, 1999.
[26] R. Lehmensiek and P. Meyer, "An efficient adaptive frequency sampling algorithm for model-based parameter estimation as applied to aggressive space mapping," *Microwave Opt. Technol. Lett.*, vol. 24, no. 1, pp. 71–78, Jan. 2000.
[27] ——, "Using efficient model-based parameter estimation for pole-free solutions of modal propagation constants, as applied to shielded planar structures," *Appl. Comput. Electromag. Soc. J.*, vol. 16, no. 1, pp. 1–10, Mar. 2001.
[28] T. J. Rivlin, *An Introduction to the Approximation of Functions*. New York: Dover, 1969.
[29] J. Stoer and R. Bulirsch, *Introduction to Numerical Analysis*. Berlin, Germany: Springer-Verlag, 1980.
[30] G. Blanch, "Numerical evaluation of continued fractions," *SIAM Rev.*, vol. 6, no. 4, pp. 383–421, Oct. 1964.
[31] A. Ralston, "Rational Chebyshev approximation," in *Mathematical Methods for Digital Computers*, A. Ralston and H. S. Wilf, Eds. New York: Wiley, 1960, vol. 2.
[32] A. Cuyt and B. Verdonk, "Multivariate reciprocal differences for branched Thiele continued fraction expansions," *J. Comput. Appl. Math.*, vol. 21, pp. 145–160, 1988.
[33] A. A. M. Cuyt and B. M. Verdonk, "A review of branched continued fraction theory for the construction of multivariate rational approximants," *Appl. Numer. Math.*, vol. 4, pp. 263–271, 1988.
[34] K. I. Kuchminskaya and W. Siemaszko, "Rational approximation and interpolation of functions by branched continued fractions," in *Rational Approximation and its Applications in Mathematics and Physics*. ser. Lecture Notes Math. 1237, J. Gilewicz, M. Pindor, and W. Siemaszko, Eds. Berlin, Germany: Springer-Verlag, 1985, pp. 24–40.
[35] W. Siemaszko, "Thiele-type branched continued fractions for two-variable functions," *J. Comput. Appl. Math.*, vol. 9, pp. 137–153, 1983.
[36] F. Oberhettinger and W. Magnus, *Anwendung der Elliptischen Funktionen in Physik und Technik*. Berlin, Germany: Springer-Verlag, 1949.
[37] T. Itoh, Ed., *Numerical Techniques for Microwave and Millimeter-Wave Passive Structures*. New York: Wiley, 1989.
[38] Y. Leviatan, P. G. Li, A. T. Adams, and J. Perini, "Single-post inductive obstacle in rectangular waveguide," *IEEE Trans. Microwave Theory Tech.*, vol. 31, pp. 806–811, Oct. 1983.

Robert Lehmensiek (S'98) was born in Swakopmund, Namibia, in 1970. He received the B.Eng. and M.Eng. degrees in electrical and electronic engineering from the University of Stellenbosch, Stellenbosch, South Africa, in 1992 and 1995, respectively, and is currently working toward the Ph.D. degree at the University of Stellenbosch.

In June 1995, he joined Reutech Radar Systems, Stellenbosch, South Africa, where he has been mainly involved with the development of passive microwave components including phased-array antennas. His main interests include optimization methods and computer-aided design and modeling of passive microwave circuits.

Petrie Meyer (S'87–M'88) received the M.Eng and Ph.D. degrees from the University of Stellenbosch, Stellenbosch, South Africa, in 1988 and 1995, respectively.

In 1988, he joined the Department of Electrical and Electronic Engineering, University of Stellenbosch, where he is currently an Associate Professor. His main interest is design and analysis algorithms for passive microwave circuits and computer-aided design (CAD), and include hybrid numerical electromagnetic (EM) techniques, mathematical device models, and optimization.

Dr. Meyer was section chair for the IEEE South African Section in 1997 and technical chair for the 1999 IEEE Region 8 AFRICON conference.